



# The Grell-Freitas Convection Parameterization: Recent Developments and Applications within the NASA GEOS Global Model

Saulo R. Freitas<sup>1,2</sup>, Georg Grell<sup>3</sup>, Andrea Molod<sup>2</sup>, and Matthew A. Thompson<sup>2,4</sup>  
 (1) Universities Space Research Association, Columbia, MD, USA. (2) Global Modeling and Assimilation Office, NASA/GSFC, Greenbelt, MD, USA  
 (3) National Oceanic and Atmospheric Administration, Boulder, CO, USA.. (4) Science Systems and Applications Inc., Lanham, MD, USA



AGU FM 2017: A31E-2240

**1. Introduction**  
 We implemented and began to evaluate an alternative convection parameterization for the NASA Goddard Earth Observing System (GEOS) global model. The parameterization (Grell and Freitas, 2014, hereafter GF) is based on the mass flux approach with several closures, for equilibrium and non-equilibrium convection, and includes scale and aerosol awareness functionalities. Recently, the scheme has been extended to a tri-modal spectral size approach to simulate the transition from shallow, congestus, and deep convection regimes. In addition, the inclusion of a new closure for non-equilibrium convection resulted in a substantial gain of realism in model simulation of the diurnal cycle of convection over the land.

**2. Brief Description of the GF Convection Parameterization**  
 The GF scheme is based on the mass flux approach with the following main features:  
 • Scale awareness through Arakawa et al. (2011) approach,  
 • Aerosol dependence through auto-conversion and evaporation formulations depending on the environmental cloud concentration nuclei.  
 • A tri-modal formulation, which allows up to three plumes representing the main convective modes existing in a tropical environment (Johnson et al., 1999): shallow, congestus, and deep plumes.  
 • A set of closures to determine the mass flux at the cloud base to adequately account for the diverse regimes of convection in a given grid cell.  
 • Transport of momentum, tracers, water, and moist static energy.  
 • Application of probability density functions to emulate the vertical mass flux profiles, providing an effective method to set the vertical distribution of heat and mass, which is very useful for fine-tuning the model.  
 • A closure for non-equilibrium convection adapted from Bechtold et al. (2014).

**3. A Scale Aware Convection Parameterization**  
 In GF, the scale dependence for deep convection is designed using the method described by Arakawa et al. (2011), who proposed the following equation for the vertical eddy transport that includes the scale dependence through  $\sigma$  parameter:  

$$\overline{w'\phi'} = (1 - \sigma) \overline{w'\phi'}_{adj} + \sigma \overline{w'\phi'}_{adj}$$
 Vertical eddy transport. Fractional area covered by the active cloud draft. Eddy transport given by a conventional CP for a full adjustment to a quasi-equilibrium state.  
 In GF,  $\sigma$  is simply determined by the ratio between the initial entrainment rate (converted to an effective radius size of the updraft) and the local grid cell area:  
 • at low resolution ( $\sigma \rightarrow 0$ ), the conventional parameterization built-in the GF scheme dominates.  
 • at high resolution ( $\sigma \rightarrow 1$ ), the parameterization gives way to the microphysics scheme, assuring a smooth transition from the non-resolved to the resolved scales.

**4. GF Scale Dependence Results with the NASA GEOS-5 Global Model**  
 We explored the GF scale-dependence approach by performing a cascade of global scale simulations with uniform spatial resolution, varying from approximately 50 km down to 6 km.  
 • Figure 1 introduces model results of the simulated total precipitation (left column) and from the convection parameterization (CP) only (right side). These results correspond to a 3-day average in mm/day and from top to bottom, model resolution increases from c180 to c1440 (see Table 1).  
 • On the left side of Figure 1, the total precipitation field becomes richer in details with filamentary structures, while preserving the broader pattern and spatial distribution, with the global mean oscillating between 3.17 and 3.28 mm/day.  
 • On the right side of Figure 1, at low resolution, CP dominates the generation of rainfall, mainly over the tropical region, but gradually reduces its participation as the model resolution increases. The CP global mean shows a monotonic decrease from 1.75 mm/day at c180 to 0.53 mm/day at the highest resolution here applied (6 km).

**5. Improving the Simulation of the Diurnal Cycle of Convection in GF Scheme**  
 In the attempt to improve the diurnal cycle in the GF scheme, we adopted a closure for non-equilibrium convection developed by Bechtold et al. (2014, hereafter B2014), which as we further demonstrate, notably improves the simulation of the diurnal cycle of convection and precipitation over the land. B2014 proposed the following equation for the convective tendency for deep convection:  

$$\frac{\partial A}{\partial t}_{non-eq} = - \left( \frac{A}{\tau} - \tau_{BL} \frac{\partial A}{\partial z} \right)$$
 where A is called density-weight buoyancy integral, and  $\tau$  and  $\tau_{BL}$  are appropriated time scales. The tendency on the right side of this equation, is the total boundary layer production given by:  

$$\frac{\partial A}{\partial t}_{BL} = - \frac{1}{T} \int_{P_{surf}}^P \rho_{base} \frac{\partial T}{\partial z} dp$$
 $T^*$  is a scale temperature parameter with a range of about 1 to 4 K.  
 The GF scheme now includes a diurnal cycle closure adapting the concept introduced by B2014. Results obtained with the GEOS model configured both as a time-dependent single column model (SCM) as well as a fully 3-D global model, are shown in the following discussions.

**GF Scale Dependence in the NASA GEOS Model**

GEOS Model horizontal resolution	Global Mean			
	Precipitation (mm/day)		Fraction (parameterized /total)	
	Parameterized	Total		
C180	~ 50km	1.75	3.19	55%
C360	~ 25km	1.59	3.20	50%
C720	~ 12km	1.19	3.17	38%
C1000	~ 09km	0.84	3.23	26%
C1440	~ 06km	0.53	3.28	16%

Table 1. Summary of the GF scale dependence within NASA GEOS global model.

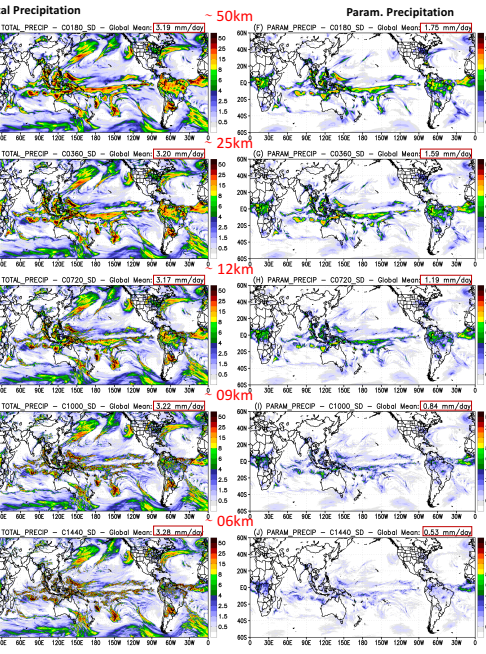


Figure 1. Total precipitation (left) and from the convective parameterization only (right) averaged over 3-day run. From top to bottom, model resolution increases from c180 (~ 50 km) to c1440 (~ 6 km). The global mean in mm/day appears on top of each panel.

**6. Discussion of Figures 2 and 3**  
 GEOS AGCM with the GF ran as a single column model for 24 January to 25 February 1999 using the forcing 'TRMM\_LBA' for a site over the Amazon Basin.

• Figure 2 shows composites of the diurnal cycle of the vertical mass flux of the three plumes as well as total and convective precipitation. The tri-modal plumes are depicted by uniform colors to define their spatial and temporal occurrences. In Panel (A), without applying the diurnal cycle closure, the three convective modes coexist and are triggered just a few hours after the sunrise, with the deep convection occurring too early and producing a maximum of precipitation about 15 UTC (approximately ~ 11 AM). A clear separation between the convective modes is observed when the diurnal cycle closure is applied (Panel B), reducing the amount of potential instability available for the deep convection. In this case, the precipitation from the deep penetrative convection is delayed (green contour) with the maximum rate taking place between 18 and 21 UTC, more consistent with the observations of the diurnal cycle over the Amazon region.  
 • Figure 3 presents the same results as Figure 2 but applying the grid-scale vertical moistening tendency associated with the three convective modes. Panel A shows the net effect (moistening minus drying) of the competition of the 3 plumes. Including this closure, a much smooth transition is simulated with a late morning and early afternoon low/mid tropospheric moistening by shallow and mid plumes, followed by a late afternoon and early evening tropospheric drying by the rainfall from the deep cumulus.

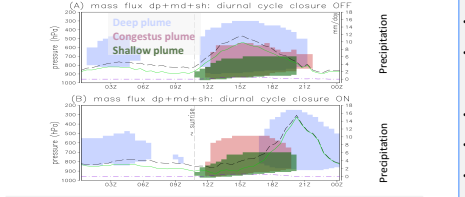


Figure 2. Time average of the diurnal cycle of the vertical mass flux of the three convective plumes (shaded: green, light red, and light blue represents shallow, mid, and deep, respectively) and precipitation (contour: black, green and purple represents the total, and the convective from deep and mid plumes, respectively). The scale for precipitation appears on the right axis in mm/day. Panel A (B) represents the results without (with) the diurnal cycle closure.

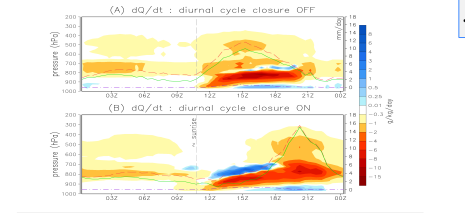


Figure 3. Time average of the diurnal cycle of the grid-scale vertical moistening tendency associated with the three convective modes (shaded) and precipitation (contour: red, green and purple represents the total precipitation, and the convective from deep and mid plumes, respectively).

**7. Applications of the Diurnal Cycle Closure on Fully 3-D Global Scale Simulations with the NASA GEOS Model**  
 • C360 spatial resolution (~25km) for July 2015 and January 2016  
 • Datasets: Global Precipitation Climatology Project (GPCP v2.1), the Precipitation Estimation from Remotely Sensed Information using Artificial Neural Networks (PERSIANN), the NOAA CPC Morphing Technique (CMORPH), the TRMM Multi-satellite Precipitation Analysis (TMPA) and the Global Precipitation Measurement (GPM).  
 • Monthly and spatial domain averages of the diurnal cycle of precipitation.  
 • The total precipitation (GF\_TT) and from the CP only (GF\_CN, dashed curves) are presented for model results.

**8. Discussion of Figure 4**  
 • A global perspective of the precipitation simulation with GEOS\_GF and the impact of the diurnal cycle closure is provided by Figure 4 for January 2016.  
 • Figure 4 shows the monthly average of the diurnal cycle of the precipitation over land (column A) and ocean (column B) areas as estimated by the TRMM and simulated by the GEOS\_GF, including or not the diurnal cycle closure.  
 • TRMM estimation evidences two peaks of precipitation: a nocturnal one around 3 AM over oceans and another one in late afternoon (3 to 6 PM) over land.  
 • Both simulations with model GEOS\_GF seem to perform well in terms of the precipitation amount, mainly over oceans.  
 • Over land (column A) the simulation with the diurnal cycle closure is superior with a better representation of the morning to early afternoon gap of precipitation, in all continents: Africa, Australia and Amazonia.

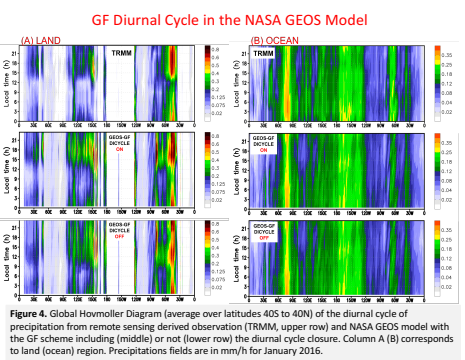


Figure 4. Global Homovler Diagram (average over latitudes 40S to 40N) of the diurnal cycle of precipitation from remote sensing derived observation (TRMM, upper row) and NASA GEOS model with the GF scheme including (middle) or not (lower) row the diurnal cycle closure. Column A (B) corresponds to land (ocean) region. Precipitations fields are in mm/h for January 2016.

**9. Discussion of Figures 5 and 6**  
 • GPCP estimates gross monthly mean of 0.349 and 0.108 mm/h for each month over the Amazon Basin (Fig. 5 A) and CONUS (Fig. 6 A), respectively.  
 • We explore the intradiurnal estimation from TRMM, GPM, and CMORPH to provide the average diurnal cycle. Observe that for the Amazon Basin case (Fig. 5 A), they agree very well concerning the phase, with the minimum rate around noon and peaking between 3 to 6 PM. For the intensity, they inform daily mean rates of 0.338, 0.339 and 0.281 mm/h, respectively.  
 • Among the five estimates, GPCP, TRMM, and GPM are very close, while CMORPH and PERSIANN have the lower and higher values.  
 • Results with GEOS model with GF scheme are shown with (DC1, red colors) or not (DC0, green colors) the diurnal cycle closure.  
 • For Amazon Basin (Fig. 5 A), both have monthly average precipitation (0.353 and 0.384, respectively) in the range of the estimates based on observations. Note also that the model simulation precipitation DC1 stands closer to the central range of the observations.  
 • In regards of the phase of the modeled diurnal cycle, good agreement with the available observations is attained with this closure.  
 • Model precipitation for the case DC0 starts to increase just around 9h LT, a few hours after sunrise, and peaks about noon. The inclusion of the diurnal cycle closure (case DC1), causes a delay of about 3 hours, with the rain rate peaking about 3 to 6 PM, much closer to the observations.  
 • The others domains and time period have similar findings.

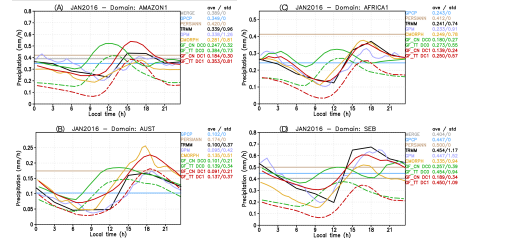


Figure 5. Diurnal cycle of precipitation from remote sensing derived observations and NASA GEOS model with the GF scheme. Panel A) shows results for the Amazon Basin, (B) for Central Africa, (C) for Australia, and (D) for Southeast region of Brazil on Jan 2016. Model results are shown in terms of total precipitation (GF\_TT) and only from GF convection parameterization (GF\_CN and dashed lines). Models results in red and green colors correspond to simulations including or not the diurnal cycle closure, respectively.

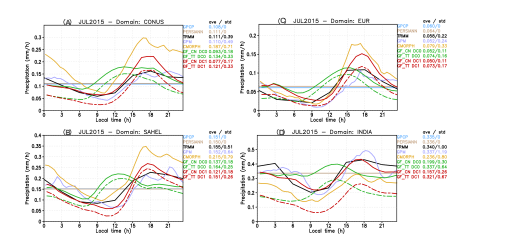


Figure 6. Diurnal cycle of precipitation from remote sensing derived observations and NASA GEOS model with the GF scheme. Panel A) shows results for the Continental US, (B) for Europe region, (C) for Sahel, and (D) for India on July 2015. Model results are shown in terms of total precipitation (GF\_TT) and only from GF convection parameterization (GF\_CN and dashed lines). Models results in red and green colors correspond to simulations including or not the diurnal cycle closure, respectively.

**10. Summary**  
 An alternative convection parameterization described in Grell and Freitas (2014) with recent developments was implemented in the NASA GEOS-5 modeling and assimilation system. In this paper, we introduced two main features of GF, which we expect will be useful in applications of the NASA GEOS global model:  
 • the scale dependence approach, which seems to work as expected for a cascade of simulations with increasing uniform grid resolution, as it provides a smooth transition from non-resolved to resolved cloud scales, and  
 • the tri-modal plume design with a diurnal cycle closure, which appears to be a consistent route to address the problem of simulating the transition from shallow to deep and precipitating convection regimes over the land, in the context of sub-grid scale parameterizations.  
 The planned next steps consist of a comprehensive quantitative evaluation of the NASA GEOS global model with GF for weather and seasonal scale applications.  
**References**  
 Arakawa, A., J.-H. Jung, and C.-M. Wu. Toward unification of the multiscale modeling of the atmosphere, *Atmos. Chem. Phys.*, 11, 3731-3742, doi:10.5194/acp-11-3731-2011, 2011.  
 Bechtold, P., N. Semane, P. Lopez, J. Chaboureau, A. Beljaars, and N. Bornmann: Representing Equilibrium and Nonequilibrium Convection in Large-Scale Models, *J. Atmos. Sci.*, 71, 734-753, doi: 10.1175/JAS-D-13-0163.1, 2014.  
 Grell, G. A. and D. Devenyi: A generalized approach to parameterizing convection combining ensemble and data assimilation techniques, *Geophys. Res. Lett.*, 29, 38-1-38-4, doi:10.1029/2002GL015311, 2002.  
 Grell, G. A. and S. R. Freitas: A scale and aerosol aware stochastic convective parameterization for weather and air quality modeling, *Atmos. Chem. Phys.*, 14, 5233-5250, doi:10.5194/acp-14-5233-2014, 2014.  
 Johnson, R.H., T. M. Rickenbach, S. A. Rutledge, P. E. Oesikeleski, and W. H. Schubert: Tri-modal Characteristics of Tropical Convection, *J. Climate*, 12, 2397-2418, doi: 10.1175/1520-0442.1999